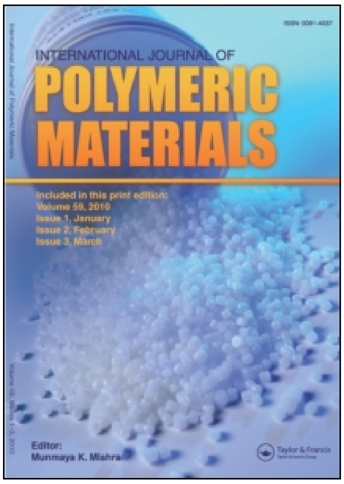

International Journal of Polymeric Materials
Publication details, including instructions for authors and subscription information:
http://www.informaworld.com/smpp/title~content=t713647664

Crystallinity Effects on Fracture of Rings Made of Thermoplastic Powder Impregnated Carbon or Glass Fiber Composites

M. Evstatiev[a]; K. Friedrich[b]; S. Fakirov[a]
[a] Laboratory on Structure and Properties of Polymers, RSofia University, Sofia, Bulgaria [b] Institute for Composite Materials (Ltd.), University of Kaiserslautern, Kaiserslautern, Germany

To cite this Article Evstatiev, M. , Friedrich, K. and Fakirov, S.(1993) 'Crystallinity Effects on Fracture of Rings Made of Thermoplastic Powder Impregnated Carbon or Glass Fiber Composites', International Journal of Polymeric Materials, 21: 3, 177 — 187

To link to this Article: DOI: 10.1080/00914039308012045

URL: http://dx.doi.org/10.1080/00914039308012045

Intern. J. Polymeric Mater., 1993, Vol. 21, pp. 177–187
Reprints available directly from the publisher
Photocopying permitted by license only

Printed in Malaysia

Crystallinity Effects on Fracture of Rings Made of Thermoplastic Powder Impregnated Carbon or Glass Fiber Composites

M. EVSTATIEV,† K. FRIEDRICH‡ and S. FAKIROV†

†Sofia University, Laboratory on Structure and Properties of Polymers, 1126 Sofia, Bulgaria; and
‡Institute for Composite Materials (Ltd.), University of Kaiserslautern,
6750 Kaiserslautern, Germany

(Received December 3, 1992)

Effects of the supermolecular structure of a thermoplastic matrix on the flexural response of glass (GF) or carbon fiber (CF)/polyamide 12 (PA 12) composite rings were investigated. An additional attempt was made to determine their interlaminar mode I fracture energy. Specimen rings were prepared by dry winding of carbon or glass fibers bundles, interspersed with polyamide powder and surrounded by a polymer sheath, around a metallic core. The consolidation was carried out by a compression molding process. Different morphologies in the polymer matrix of the GF/PA 12 and CF/PA 12 composites were achieved by varying the cooling rate after consolidation of the material in melt and by further thermal treatment. The morphology was studied by DSC and WAXS.

KEY WORDS Composite matrix morphology, polyamide 12, continuous carbon and glass fibers, crystallinity, flexural response, interlaminar fracture toughness

I. INTRODUCTION

It is well known that the usefulness a composite material for many structural applications is often dependent on the toughness of the material in general and the interlaminar fracture toughness in particular. In order to improve the interlaminar fracture toughness and the delamination resistance of composites, thermoplastic polymers are frequently used as matrix materials.[1] Besides this important function, the major role of the matrix in fibrous composites is mainly to transfer the load between the reinforcing fibers and to protect them during processing into useful shapes.

Processing of semicrystalline thermoplastic matrix composites is usually performed by heating the parts up to a few degrees above the matrix melting point. Then, the molten matrix composite can be formed using an appropriate technique (e.g. thermoforming, pultrusion, filament winding, welding, etc.). Finally, the product is cooled down to room temperature. By controlling the cooling rate, changes in the matrix morphology can be achieved and hence different matrix toughness may be obtained. The type of the reinforcing component also influences substantially the structure of the polymer matrix, mainly due to its heterogenic nucleation effect (better expressed by carbon fibers).

In this study powder impregnated fibers as an intermediate material form were used in the preparation of unidirectional fiber reinforced ring specimens. By varying the cooling rate after consolidation of the material and by further carrying out additional thermal treatments, a different structure of carbon or glass fiber reinforced polyamide 12 was achieved in the composite matrix. The influence of these matrix structures on the physical and mechanical properties of the composite materials was followed. Preliminary studies in this respect[2,3] were already carried out for CF/PA 12 and GF/PA 12 flat specimens.

II. EXPERIMENTAL

II.1. Material and Specimen Preparation

The materials studied were thermoplastic powder impregnated fiber bundles, surrounded by a thin polymeric sheath (laboratory product of ENICHEM, Italy). Consolidation of this intermediate material form into reinforced ring specimens was carried out in a hot press, using a circular steel mold with a fixed inner diameter of ϕ_i = 80 mm and various outer diameters of ϕ_0 = 90, 100 or 110 mm, respectively (Figure 1). The following steps were performed: (a) 4 m of GF/PA 12 (tex 2400) or 12 m of CF/PA 12 (tex 800) materials were wound densely around the cylindrical core of the mold; (b) an external ring was fixed by means of screws to the basic

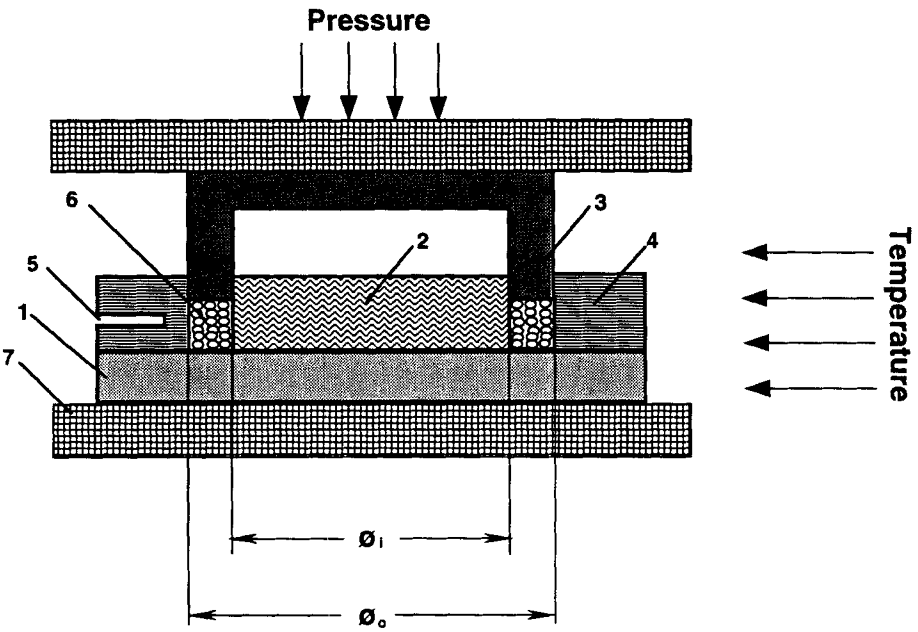

FIGURE 1 Geometry of the steel mold used for consolidation of the intermediate materials via melt into reinforced rings; 1-basic ring; 2-core; 3-plunger; 4-external ring; 5-temperature recorder of the mold; 6-composite materials; 7-press plates.

ring and the plunger was placed; (c) the mold was heated in a hydraulic press up to 210°C (the temperature of the mold was recorded rather than that of the heating plates); (d) after reaching the desired temperature, a pressure of 5.5 MPa was applied for 5 minutes; (e) by varying the cooling rate, the following specimen series were obtained:

Series A—rapid cooling at a rate of 180–190° C/min without pressure
Series B—slow cooling under pressure at a rate of 7–80°C/min
Series C—specimens of series B were heated additionally at 150°C for 3 hours without pressure.

Specimens with ϕ_i = 80 mm and ϕ_0 = 100 or 110 mm were prepared in the same manner using 8 or 12 m GF- and 30 or 50 m of CF-polymer bundles, respectively. In order to avoid sticking of the specimens to the mold walls, silicon spray was used.

II.2. Structural Characterization

The microstructure and morphology of different GF or CF containing specimens (A, B and C) were studied by WAXS and DSC.

The DSC measurements were performed on a Mettler TA 3000 apparatus at a scanning rate of 10°C/min during heating and cooling. From the melting and crystallization peaks, the degree of crystallinity (W_C) and the mass fraction (X_C), respectively, were determined after isothermal (T_c = 160°C) crystallization from the melt. Use was made of the equation $W_C = \Delta H_m/\Delta H^0$ and $X_C = \Delta H_c/\Delta H^0$ where ΔH_m is the heat of fusion and ΔH_c is the heat of crystallization; the term ΔH^0 is the theoretical heat of fusion and was read from the literature as 134 kJ/kg.[5] The relationship between the crystallinity mass fractions (W_C or X_C) and the crystallinity volume fractions (W_{CV} or X_{CV}) is $W_{CV} = W_C\rho_C/(\rho_C - W_C(\rho_C - \rho_A))$, where the density of the crystalline and the amorphous PA 12 phases were ρ_C = 1.10 kg/m^3 and ρ_A = 0.99 kg/m^3, respectively.[6]

Wide angle X-ray scattering (WAXS) measurements were made on a D 500 Siemens diffractometer, using Ni-filtered CuKα radiation. The crystallite size was estimated from the transmission meridional diffractograms of the samples by applying the Scherrer equation.[7]

II.3. Mechanical Tests

III.3.1. Flexural response. Before the actual tests, rings were cut into four equal parts (quarters). The rings used for these tests had the following diameters: ϕ_i = 80 mm and ϕ_0 = 90, 100 or 110 mm, respectively, and they possessed a height (h) of about 5 mm for each of the series A, B and C. With these segments, flexural tests were carried out on a device proposed by Chang[8] using a Zwick 1464 machine (Figure 2), at room temperature and a cross-head speed of 2 mm/min. The results for each series were averaged from five measurements.

II.3.2. Mode I double cantilever beam (DCB). Since it was not possible to create a starter crack during the manufacturing process of the rings, this crack was made afterwards in the following manner: a slot was made in the middle of one end of the ring quarters by means of a saw. This slot was 1 mm wide and 5 mm

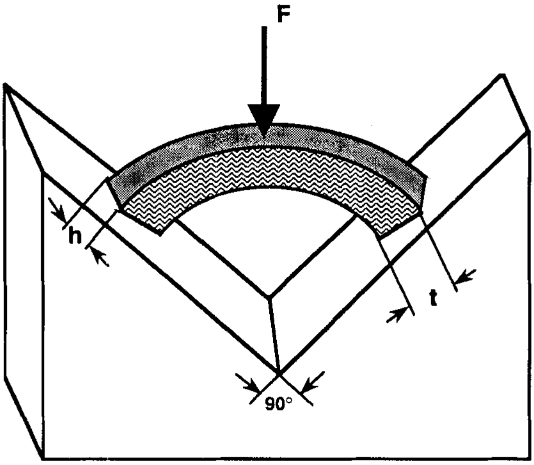

FIGURE 2 Device for 3PB test with a 90 degree arc angle.

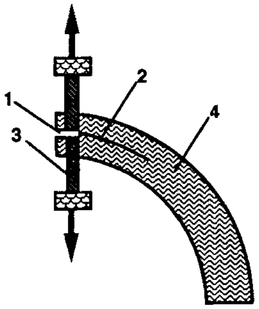

FIGURE 3 Test geometry for the DCB (mode I) test: 1-slot; 2-starter crack; 3-hinges; 4 ring quater.

deep. Then, by the use of a very thin razor blade, the depth of the slot was increased additionally to 15–20 mm. Thus the starter crack amounted to one third of the specimen's (ring quarter) length. Load was applied at a cross-head speed of 1 mm/min via hinges, 3 mm wide placed in the original saw cut slot (Figure 3).

The specimen was loaded continuously and the crack lengths were marked every 5-6 mm until the crack had propagated over a length of 45-50 mm. The results were averaged from five measurements using the following equation: $G_{IC} = 3P\delta/2ha$, where P is the load [N], δ the displacement [mm] and "a" the crack length [mm].[9]

III. RESULTS

III.1. Microstructure

Table I shows data of DSC and WAXS measurements of (a) the single GF- and CF-polymer bundles, and (b) the GF/PA 12 and CF/PA 12 composites. It can be seen that the rapidly cooled CF- or GF-containing composites (series A) as well

TABLE I

DSC and WAXS data of GF- and CF-polymer bundles, and of GF/PA 12 and CF/PA 12 composite rings

Specimens	Series	T′ (°C)	T″ (°C)	Wcv (DSC)	Xcv (DSC)	D (A)
GF-bundle		-	178	0.44	0.39	-
CF-bundle		-	181	0.55	0.52	-
GF/PA 12	A	-	180	0.35	0.31	77
	B	172	181	0.29	0.27	88
	C	173	180	0.30	0.26	95
CF/PA 12	A	-	180	0.42	0.39	37
	B	172	181	0.37	0.32	41
	C	172	181	0.36	0.34	40

as the CF- and GF-bundle materials reveal one melting peak (T_m = 180°C). The slowly cooled (B series) and additionally annealed (series C) GF/PA 12 and CF/PA 12 composites show, on the other hand, two peaks at 170 and 180°C. These experimental results, as well as the broad melting temperature ranges (158–187°C) observed with the GF/PA 12 and CF/PA 12 samples of series A suggest the presence of various crystalline arrays, which differ in size and perfection, as a function of thermal treatment of these composites. The volume fractions of the crystalline phases (W_{CV} and X_{CV}) of the CF-containing composites, as calculated on the basis of the heats of fusion and exotherms after melting and isothermal crystallization at 160°C, are higher than those of the GF/PA 12 (Table I). Furthermore, the values of W_{CV} are very close to those of W_{CV} of the respective series A, B and C of the GF/PA 12 and CF/PA 12 laminates. In addition, the GF- and CF-bundle materials show considerably higher values of X_{CV} and W_{CV} than the composites (by 35–45% and 40–60%, respectively, Table I).

Table I and Figure 4 show also that for both types of composites (GF/PA 12 and CF/PA 12) the crystalline volume fractions (W_{CV} and X_{CV}) slightly decrease with a transition from series A to B, but they remain nearly constant from B to C. On the opposite, an increase is observed for the crystallite size (D) when going from A to C. This is however, only clearly visible for the GF/PA 12 composites, for which, in addition, the D-values are much greater than for CF/PA 12 rings (Figure 4).

III.2. Flexural Response

Flexural response data of GF/PA 12 and CF/PA 12 composite rings segments of different thickness (5, 10 and 15 mm) are summarized in Tables II and III. Regardless of a slightly greater height (h) of series A specimens (by about 0.6 mm), the F_{max} values obtained with this series are considerably lower than those of specimens from the B and C series. The same trend is even more clearly observed for the F_{max}/h ratios (Tables II, III, and Figure 5). On the other hand, the deformation ability (deflection) of samples from series A is clearly higher than that of samples from series B and C. The double and triple increase of the sample thickness

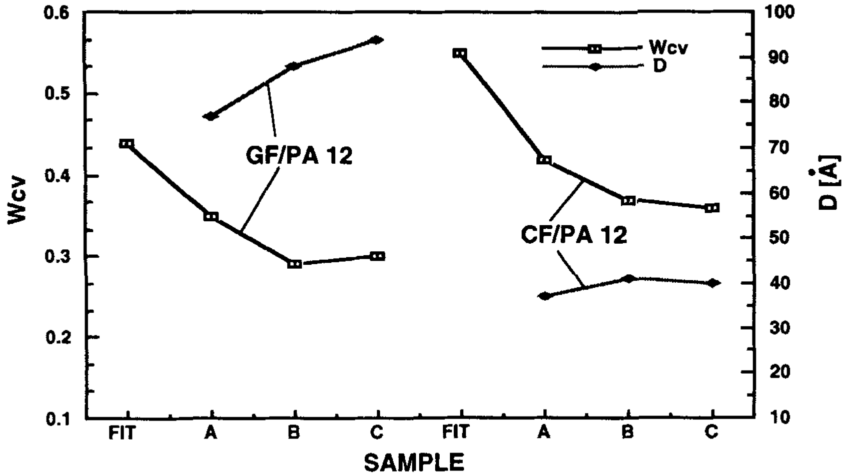

FIGURE 4 Degree of crystallinity (W_{CV}) and crystalline size (D) of the PA 12 matrix as a function of thermal pre-history of GF- and CF/PA 12 laminates.

TABLE II

Flexural response data of GF/PA 12 composite ring segments.

Ring Dimensions (mm)	Specimens (Series)	F_{max} (N)	Deflection at Break (mm)	F_{max}/h (N/mm)	Shrinkage after Cutting (mm)
$\emptyset_i = 80$	A	398	7.0	86	0.8
$\emptyset_o = 90$	B	509	4.2	108	2.0
	C	556	3.9	121	2.1
$\emptyset_i = 80$	A	1090	9.1	218	1.3
$\emptyset_o = 100$	B	1304	6.6	282	2.1
	C	1330	6.3	283	2.2
$\emptyset_i = 80$	A	1860	8.8	320	1.2
$\emptyset_o = 110$	B	2676	4.9	497	2.2
	C	2460	4.8	490	2.1

(ϕ_0 = 90, 100 or 110 mm) leads to an increase of the F_{max}/h ratios by factors of 2.5 and 4.5 for GF/PA 12, respectively, and by 3 and 5 for the CF/PA 12 composite system.

The existence of internal stresses was established in all samples as it can be deduced by the shrinkage of the rings after their cutting (Tables II, III, and Figure 6). These internal stresses are greatest in the case of CF/PA 12 laminates. In addition, samples of series A of both composite systems show stresses that are two times lower than those measured for the B and C series.

III.3. Mode I Double Cantilever Beam

During the mode I fracture toughness tests, it was observed that the crack propagation was very stable when testing samples of series A, a slight tendency for

TABLE III

Flexural response data of CF/PA 12 composite ring segments

Ring Dimenasions (mm)	Specimens (Series)	F_{max} (N)	Deflection at Break (mm)	F_{max}/h (N/mm)	Shrinkage after Cutting (mm)
$\varnothing_i = 80$	A	582	5.8	111	1.4
$\varnothing_o = 90$	B	758	3.6	152	2.3
	C	732	3.3	166	2.8
$\varnothing_i = 80$	A	1877	8.0	341	1.4
$\varnothing_o = 100$	B	2180	4.0	481	2.6
	C	2297	4.1	489	2.5
$\varnothing_i = 80$	A	3108	7.6	546	1.7
$\varnothing_o = 110$	B	3808	4.4	762	2.5
	C	3816	4.1	763	2.8

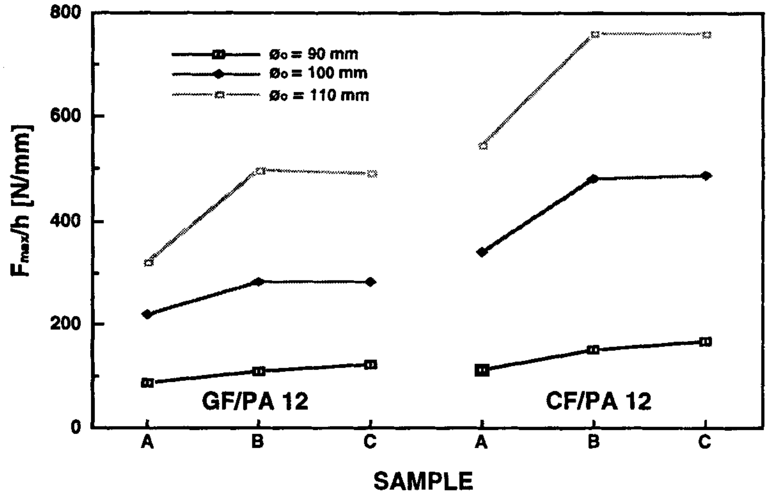

FIGURE 5 Flexural response data (F_{max}/h) of GF- and CF/PA 12 composite ring segments.

crack instability occurred for samples of types B and C (Figures 7(a) and (b)). Regardless of the crack advance, a large number of fibers bridging the crack was observed in all samples (Figure 8). In the same figure one can see that during the tests side cracks also appear and propagate non-uniformly at both sides of sample. This is most probably due to crossing of bundles during consolidation in the mold and for this reason the correct determination of the mode I (G_{IC}) values is almost impossible. Nevertheless, a tendency of higher G_{IC} observed for the B and C series of CF/PA 12 samples, whereas a decrease of G_{IC} seems to occur in the order from A to C series in the case of GF/PA 12 laminates. The same trend was observed in our previous study on CF/PA 12 and GF/PA 12 flat laminates.[2,3]

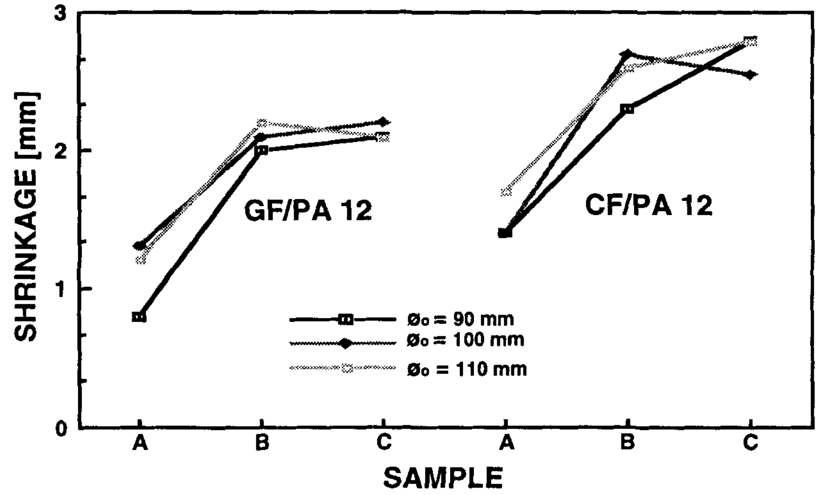

FIGURE 6 Shrinkage of the GF- and CF/PA rings after their cutting.

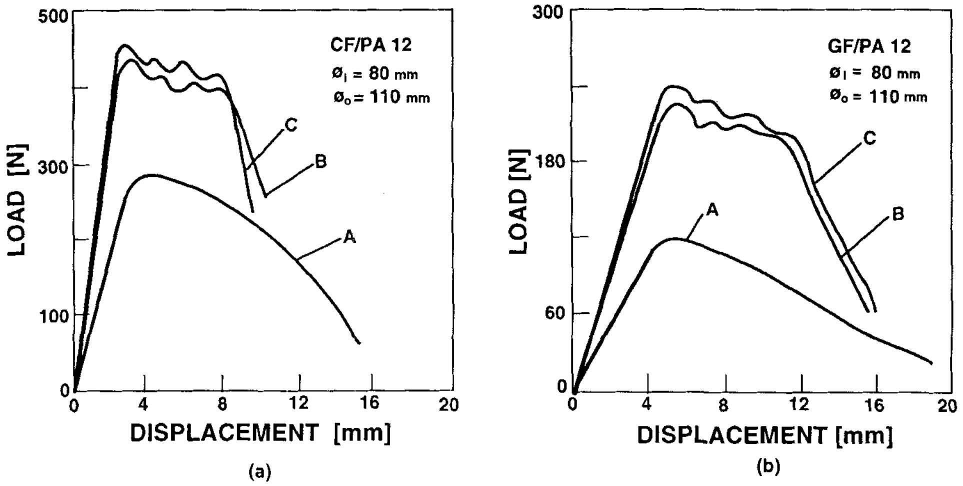

(a) (b)

FIGURE 7 Load-displacement plot in mode I loading conditions: (a) CF/PA 12 composite system; and (b) GF/PA 12 composite system.

IV. DISCUSSION

On the basis of the data presented in Table I for the volume fractions of crystallites before melting (W_{CV}) and after isothermal crystallization (at 160°C) from the melt (X_{CV}) as well as for the mean size of the crystallites (D), the conclusion can be drawn that the main structure-determinant factor is the type of the reinforcing elements, while the thermal pre-history of the samples is of secondary importance. Reasons for this statement are: (a) the high crystallization ability of polyamide 12 and, (b) the difference in the nucleation ability of the glass and carbon fibers.

The high nucleation ability of carbon fibers provides the possibility of growth of

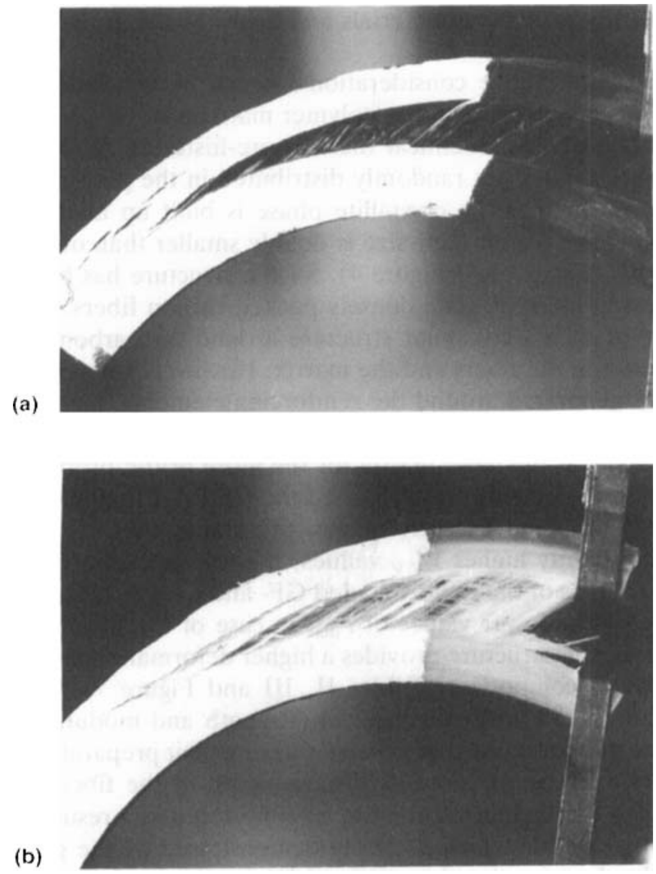

FIGURE 8 Crack propagation, secondary crack formation and fibers bridging the crack during a mode I fracture toughness test: (a) CF/PA 12 composite system; and (b) GF/PA 12 composite system.

crystallites around the fibers (the so-called transcrystallization). These crystalline arrays differ in morphology from the spherulites arising in the bulk of the polymer matrix.[10-12] On the other hand, due to their insignificant nucleation effect, transcrystallization is very seldomly observed with glass fibers.[13,14] The higher values of W_{CV} and X_{CV} of CF/PA 12 samples as compared to those of the glass fiber containing samples (Table I) indicated the stronger nucleation effect of carbon fibers.

Taking into account the fact that the mean crystallite size after additional thermal treatment of the GF/PA 12 and CF/PA 12 samples remains practically unchanged (Table I and Figure 4, series C and B), it can be assumed that the densely packed reinforcing fibers in the composite materials hamper the crystallite growth. This effect is more clearly expressed in the samples containing carbon fibers, probably due to the smaller diameter of CF as compared to that of GF and hence to the denser packing of carbon fibers. An additional confirmation of the stearic effect of the reinforcing element can be found in the considerably lower values of W_{CV} and X_{CV} in GF/PA 12 and CF/PA 12 samples as compared to those of GF- and CF-bundle materials. These differences are due to the less dense distribution and alignment of the fibers in these materials and hence to the greater free volume in the polymeric matrix.

On the basis of the above considerations, it can be concluded that a certain morphological difference exists in the polymer matrices of GF- and CF-containing samples, regardless of their identical thermal pre-histories. While in the GF/PA 12 samples the crystallites are randomly distributed in the polymer matrix, in the case of CF/PA 12 samples the crystallite phase is built up mainly of crystalline layers surrounding the fibers; their size is doubly smaller than observed with GF/PA 12 composites (Table I and Figure 4). Such a structure has been observed by other researchers in cases of quite densely packed carbon fibers.[15]

The presence of such a columnar structure around the carbon fibers improves the adhesion between the fibers and the matrix. However, when mostly transcrystalline layers are generated around the reinforcing elements, and when the bonds between the fibers and the matrix are rather strong, a brittle fracture of the matrix may take place. This is the basic reason for the more brittle properties of the CF/PA 12 composites, in comparison to those of the GF/PA 12 samples; Tables II and III as well as Figures 5 and 7 clearly suggest this assumption.

In spite of the slightly higher W_{CV} vallues, the less perfect crystallite structure and the lower D values of the rapidly cooled GF- and CF/PA 12 samples (A series) are the reasons for the lower values of $F_{\max}$ in case of the flexure and G_{IC} tests. On the other hand, this structure provides a higher deformation ability (deflection) of the two types of composites (Tables II, III and Figure 7). The less perfect crystallite structures and lower mechanical (strength and modulus) properties in these samples are due to macroscopic changes during their preparation, in particular the formation of microcavities, voids, disorientation of the fibers and poor consolidation between the bundles. They can be considered as a result of the absence of pressure during cooling which is clearly demonstrated by the greater height of all samples of the A series (by about 0.6 mm).

V. CONCLUSION

In order to describe the morphological changes occurring during the processing of CF- and GF/polyamide 12 composites, the volume fraction and the size of crystallites as a function of the type of the reinforcing component and the thermal prehistory were analyzed. It could be established that due to the nucleation ability of carbon fibers, CF/PA 12 laminates show a relatively higher degree of crystallinity than GF/PA 12 composites. Carbon fibers affect the crystal structure at the fiber/matrix interface, generating transcrystalline layers around the fibers. Such a columnar structure around densely packed reinforcing components improve the fiber/matix adhesion and is also strongly reflected in the properties of the laminates. CF/PA laminates were found to possess high values of flexural forces and internal stress (deduced by the shrinkage of their rings after cutting) and a more ductile behavior than GF/PA 12 laminates.

Acknowledgments

The authors gratefully acknowledge the financial support of the German Department of Research and Technology (BMFT 227-9211-Bul, N 218.2) for collaboration between the German and Bulgarian partner institutes. Further thanks are due to ENICHEM, Italy, for free delivery of the research materials.

References

1. J. Brandt and H. Richter, *Kunststoffe*, **77**, 40 (1987).
2. H. Wittich, M. Evstatiev, E. Bozwelieva, K. Friedrich and S. Fakirov, *Adv. Compos. Mater.*, Japan **2**, 135 (1992) .
3. M. Evstatiev, K. Friedrich and S. Fakirov, *Int. J. Polym. Mater.* (1993) (in press).
4. Atochem Report, *Thermoplastic Polymers in Powders for Composites*, Atochem, Paris, 1985.
5. J. E. Stamhuis and A. J. Pennings, *Polymer*, **18**, 667 (1977).
6. *Encyclopedia of Polymer Science and Engineering*, John and Sons, New York, 1987.
7. B. D. Cullity, in *Elements of X-Ray Diffraction*, Addison-Wesley Publ., Reading, Massachusetts, 1978.
8. F. K. Chang and Z. Kutlu, *J. Mater. Sci.*, **23**, 11 (1989).
9. European Group of Fracture (EGF), Composites task group, Draft protocol for mode I and mode II testing, 1989.
10. C. M. Tung and O. J. Dynes, *J. Appl. Polym. Sci.*, **33**, 505 (1987).
11. B. Chauchard, J. Cinquin, *Macr. Chem. Macr. Symp.*, **9**, 99 (1987).
12. L. Caramaro, B. Chabert and J. Chauchard, *C.R. Acad. Sci., Paris*, **306**, 887 (1988).
13. T. Bessel and J. B. Shortall, *J. Mat. Sci. Letters*, **3**, 1071 (1984).
14. R. H. Burton and J. M. Folkes, *Plastics and Rubber Processing and Applications*, **3**, 129 (1983).
15. S. Saiello, J. Kenny and L. Nicolais, *J. Mater. Sci.*, **25**, 3493 (1990).